DOI: 10.1002/ejic.200601232

Hydrolysis of a (2-Propanol)yttrium Triiodide Complex in the Presence of Glymes: Synthesis and X-ray Structures of Hydroxo-Bridged Dinuclear Yttrium Complexes and Their Applications in Materials Science

Shashank Mishra,*[a] Stéphane Daniele,*[a] Liliane G. Hubert-Pfalzgraf,[a][†] and Erwann Jeanneau[b]

Keywords: Yttrium / Iodine / Glymes / Structure / Dinuclear complexes

The reactions of (2-propanol)yttrium triiodide, $Y(i\text{PrOH})_4I_3$, with stoichiometric amounts of water in the presence of di-, tri-, and tetraglyme yield a facile synthetic route to hydroxo-bridged, centrosymmetric dimeric yttrium complexes. These ionic derivatives, $[Y_2L_2(\mu\text{-}OH)_2(H_2O)_x(ROH)_y]I_4$ [**1**: L = triglyme, x = 2, y = 2, R = *i*Pr; **2**: L = tetraglyme, x = 2, y = 0; **3**·2EtOH: L = diglyme, x = 2, y = 4, R = Et; **4**·2EtOH: L = triglyme, x = 4, y = 0; **5**: L = tetraglyme, x = 2, y = 2, R = Et] have been characterized by elemental analysis, IR and ^{1}H NMR spectroscopy, as well as by single-crystal X-ray diffraction for **3**, **4**, and **5**. Preliminary results on the utility of these ionic derivatives as potential sources of yttrium oxide in high T_c superconductors are also presented.

Introduction

Yttrium triiodide is an attractive alternative to yttrium trifluoroacetate derivatives as a source of yttrium oxide in chemical routes to $YBa_2Cu_3O_{7-x}$ (YBCO) high T_c superconductors, because it does not form corrosive hydrofluoric acid during decomposition.[1] Hydroxo ligands are of interest in yttrium and lanthanide chemistry as reaction sites for condensation to bridged oxides[2] and as nucleophiles in RNA cleavage as well as in the catalytic hydrolysis of phosphate diesters.[3] It is generally accepted that the catalysis of phosphate diester cleavage involves substrate activation by a dinuclear lanthanide core followed by nucleophilic attack by an activated hydroxide (Scheme 1).[3] Hydroxo complexes are also often proposed as intermediates in the degradation pathways of f-element organometallic and coordination compounds.[4] Polynuclear oxo and/or hydroxo complexes of lanthanides with $[Ln_4(\mu_3\text{-}OH)_4]^{8+}$,[5] $[Ln_6(\mu_6\text{-}O)(\mu_3\text{-}OH)_8(H_2O)_{24}]^{8+}$,[6] or $[Ln_{15}(\mu_3\text{-}OH)_{20}(\mu_5\text{-}X)]^{24+}$[7] (X = halide) cores have been obtained by direct hydrolysis of lanthanide nitrates, perchlorates, or halides (chloride and iodide) in aqueous media. However, the high charge and polarizing power of lanthanides as well as the absence of any organic auxiliary ligands result in a high tendency to readily hydrolyze, thus making it difficult to control oligomerization of rare-earth centers.[8] A common synthetic strategy for controlling the advancement of hydrolysis is to introduce auxiliary ligands such as carboxylates, polyketonates, polyamines, polyols, pyridonates, alkoxides, and amino acids in the metal coordination sphere (ligand-controlled hydrolysis).[9] We have previously reported octa- and nonanuclear oxo-hydroxo yttrium species, namely $[Y_8(\mu_4\text{-}O)_2(\mu_3\text{-}OH)_4(\mu,\eta^2\text{-}AAA)_4(\eta^4\text{-}AAA)_6(\mu\text{-}OEt)_4(\mu_3\text{-}OEt)_2]$[10] and $[Y_9O_2(OH)_8(\mu,\eta^2\text{-}AAA)_8(\eta^2\text{-}AAA)_8]^-$,[11] using allylacetatoacetate $MeCOCH_2COOCH_2CH{=}CH_2$ (HAAA) as an auxiliary ligand.

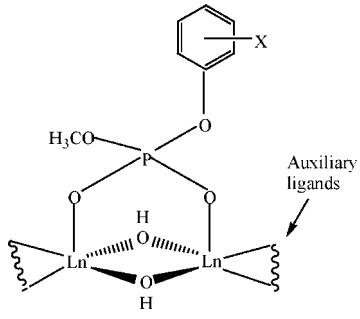

Scheme 1. A possible mechanism for the activation and cleavage of a phosphate diester substrate by a hydroxo-bridged dinuclear lanthanide species.

Although a few examples of hydroxo-bridged yttrium and lanthanide complexes with chelating ligands exist in the literature (Table 1), they have mostly been obtained from nonaqueous solutions as the result of serendipitous hydrolysis and include N-donor ligands.[12–21] The reaction conditions that lead to hydroxo formation in nonaqueous solvents have rarely been elucidated, and general synthetic pro-

[a] Université Lyon1, IRCELYON,
2 av. A. Einstein, 69626 Villeurbanne Cédex, France
Fax: +33-4-72445399
E-mail: mishrashashank74@rediffmail.com
[b] Université Lyon1, Centre de Diffractométrie,
69629 Villeurbanne Cédex, France
[†] Deceased

Table 1. X-ray crystallographically characterized dinuclear yttrium and lanthanide complexes with N- and/or O-donor ligands containing a $[Ln_2(\mu\text{-}OH)_2]$ core.

Entry	Compound[a]	Coordination environment	Ln–O(μ-OH) [Å]	Ln···Ln in dimer [Å]	Ln–μ-OH–Ln [°]	Reference
1	$[Y_2(\mu\text{-}OH)_2(H_2O)_2(\eta^6\text{-}L)_2](NO_3)_4\cdot 6H_2O$	N_6O_3	2.235(9)	3.709(3)	112.1(4)	[3b]
2	$[La_2(\mu\text{-}OH)_2(\mu,\eta^1\text{:}\eta^1\text{-}OTf)(\eta^6\text{-tpen})_2](OTf)_3\cdot 3MeCN$	N_6O_3	2.415(2)–2.421(2)	3.988(1)	111.5(8)	[21]
3	$[Yb_2(\mu\text{-}OH)_2(\eta^3\text{-bmp})_2](ClO_4)_4(HClO_4)_{0.5}(MeCN)_{7.32}(bmp)_{0.5}$	N_6O_2	2.231(4)–2.235(5)	3.656(5)	[b]	[14]
4	$[Er_2(\mu\text{-}OH)_2(\text{hexacyclen})_2](OTf)_4$	N_6O_2	2.246(2)–2.275(2)	3.802(1)	112.0(1)	[15]
5	$[Ce_2(\mu\text{-}OH)_2(MeCN)_2(H_2O)_2(\eta^4\text{-tpa})_2]I_4$	N_5O_3	2.324(7)–2.337(7)	3.829(2)	110.5(3)	[20]
6	$[Sm_2(\mu\text{-}OH)_2(N\text{-MeIm})_{10}]I_4$	N_5O_2	2.287(3)–2.309(3)	[b]	111.0(1)	[13]
7	$[Eu_2(\mu\text{-}OH)_2(\eta^4\text{-tpa})_2(OTf)_4]$	N_4O_4	2.228(2)–2.298(2)	3.715(8)	110.4(1)	[20]
8	$[Y_2(\mu\text{-}OH)_2(H_2O)_4(\eta^2\text{-phen})_4][Cl]_4\cdot 2(phen)\cdot MeOH$	N_4O_4	2.218(3)–2.233(3)	3.651(2)	110.2(2)	[12]
9	$[Tm_2(\mu\text{-}OH)_2(H_2O)_2(\eta^2\text{-phen})_4](NO_3)_4\cdot 2phen$	N_4O_4	2.204(6)–2.226(6)	3.647(1)	110.8(2)	[19]
10	$[Yb_2(\mu\text{-}OH)_2(H_2O)_2(\eta^2\text{-phen})_4](NO_3)_4\cdot 2phen$	N_4O_4	2.207(4)–2.211(4)	3.636(1)	110.7(2)	[19]
11	$[Er_2(\mu\text{-}OH)_2(H_2O)_4(\eta^2\text{-phen})_4](NO_3)_4\cdot 2phen$	N_4O_4	2.224(3)–2.247(3)	3.672(1)	110.4(1)	[18]
12	$[Lu_2(\mu\text{-}OH)_2(H_2O)_4(\eta^2\text{-phen})_4](NO_3)_4\cdot 2phen$	N_4O_4	2.201(3)–2.210(3)	3.632(1)	110.9(1)	[18]
13	$[Yb_2(\mu\text{-}OH)_2(H_2O)_2(\eta^4\text{-tmpp})_2]$	N_4O_3	2.247(7)–2.255(5)	3.724(1)	[b]	[16]
14	$[Yb_2(\mu\text{-}OH)_2(H_2O)_6(\eta^3\text{-paphy})_2]Cl_4\cdot 4H_2O$	N_3O_5	2.19(1)–2.22(1)	3.608(1)	110.0(3)	[17]
15	$[Y_2(\mu\text{-}OH)_2(H_2O)_2(EtOH)_4(\eta^3\text{-diglyme})_2]I_4\cdot 2EtOH$	O_8	2.223(6)–2.246(6)	3.684(1)	111.0(2)	this work
16	$[Y_2(\mu\text{-}OH)_2(H_2O)_4(\eta^4\text{-triglyme})_2]I_4\cdot 2EtOH$	O_8	2.237(4)–2.262(4)	3.719(1)	111.5(2)	this work
17	$[Y_2(\mu\text{-}OH)_2(H_2O)_2(EtOH)_2(\eta^4\text{-tetraglyme})_2]I_4$	O_8	2.209(7)–2.247(6)	3.710(1)	112.7(3)	this work

[a] Abbreviations: bmp = 2,6-bis(1-methylbenzimidazol-2-yl)pyridine; hexacyclen = 1,4,7,10,13,16-hexaazacyclooctadecane; L = an 18-membered hexaaza macrocycle ligand; *N*-MeIm = *N*-methylimidazole; OTf = trifluoromethanesulfonate (triflate); paphy = pyridine-2-carboxaldehyde 2′-pyridylhydrazone; phen = *o*-phenanthroline; $tmppH_2$ = 5,10,15,20-tetrakis(*p*-methoxyphenyl)porphyrin; tpa = tris(2-pyridylmethyl)amine; tpen = *N*,*N*,*N*′,*N*′-tetrakis(2-pyridylmethyl)ethylenediamine. [b] Not mentioned in the literature.

cedures for the preparation of dinuclear hydroxo complexes are lacking. In continuation of our earlier studies on the reactivity of $Y(i\text{PrOH})_4I_3$,[22,23] we wish to report in this manuscript its hydrolytic reactions in the presence of glymes. The obtained compounds **1**–**5** are the first examples of hydroxo-bridged dimeric yttrium (or lanthanide) complexes with an all-oxygen environment (Table 1). These compounds are potentially good starting materials for the synthesis of larger yttrium oxo/hydroxo clusters.[24] In addition, their utility as sources of yttrium oxide for high T_c superconductors has also been evaluated, and the preliminary results are presented in this paper.

Results and Discussion

The hydrolytic reactions of (2-propanol)yttrium triiodide, $Y(i\text{PrOH})_4I_3$, with stoichiometric amounts of water in the presence of glymes have been evaluated by using different solvents. Reactions of $Y(i\text{PrOH})_4I_3$ in toluene with triglyme or tetraglyme containing two to three equivalents of water proceed with an immediate precipitation of compounds **1** and **2** as yellow solids in good yield. The same compounds were obtained when 2-propanol was used as the reaction medium, though in lower yields because of the moderate solubility of these compounds in 2-propanol. Crystallization of these compounds from an EtOH/*n*-pentane (1:1) or EtOH/Et_2O (1:2) solution gave ethanol-solvated, hydroxo-bridged, ionic dimeric yttrium compounds **3**–**5** (Scheme 2), as established by X-ray crystallography. Similar ethanol-solvated, hydroxo-bridged dinuclear compounds were isolated in better yields by using ethanol as the reaction medium. The stability of a dinuclear $Y_2(OH)_2$ core in complexes **1**–**5** is reflected by the fact that the yttrium/glyme ratio always remained at 1:1 even if glymes were added in excess (up to 2.5 equiv.; IR and ^1H NMR evidence), the remaining coordination sites of eight-coordinated yttrium centers being filled by water and/or alcohol molecules.

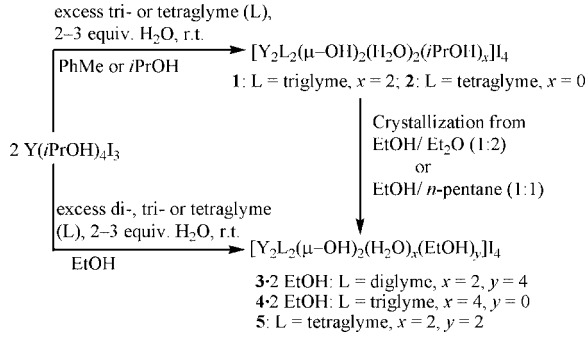

Scheme 2. Hydrolysis of $Y(i\text{PrOH})_4I_3$ in the presence of glymes.

Spectroscopic Characterization

The FT-IR spectra of **1**–**5** show the presence of alcohol functionalities as well as glyme ligands in the metal coordination sphere (Table 2). A broad strong IR absorption at 3100–3350 cm^{-1} due to ν(OH) and a weak-to-medium-intensity band at 1600–1630 cm^{-1} due to δ(OH) confirm the presence of the hydroxy functionality in **1**–**5**, the ν(Y–O) frequency appearing as medium-intensity bands in the region 400–700 cm^{-1}. The presence of di-, tri-, or tetraglyme is also confirmed by their characteristic IR absorptions. ^1H NMR spectra of compounds **1**–**5** at ambient temperature are independent of concentration and are consistent with a single-ligand environment. These spectra show peaks for the polydentate glymes, bridging hydroxy groups, and coordinated water and/or alcohol molecules in the expected

Table 2. ^{1}H NMR and IR spectroscopic data for compounds **1**–**5**.

Comp.	^{1}H NMR (CD_3CN) δ [ppm][a]				IR (Nujol) $\tilde{\nu}$ [cm^{-1}]
	μ-OH	H_2O	di-, tri-, or tetraglyme moiety	*i*PrOH/EtOH	
1	6.40 (s, 2 H)	5.2 (s, 4 H)	3 43 (s, 6 H, OMe), 3.83 (m, 14 H, OCH_2 of tetraglyme + CH of 2-propanol)	1.14 (d, J = 7.0 Hz, 12 H, Me), 3.83 (m, 14 H, OCH_2 of tetraglyme + CH of 2-propanol)	3340br ν(OH), 1610m δ(OH), 1346m, 1281m, 1249m, 1198m, 1111s, 1096s, 1077s, 1057s, 1018m, 996s, 936s, 875m, 860s, 833s, 722w, 630w, 537w, 454w ν(Y–O)
2	5.45 (s, 2 H)	5.22 (s, 4 H)	3.54 (s, 6 H, OMe), 3.80 (s, H, OCH_2), 3.90 (s, H, OCH_2)	–	3333 br ν(OH), 1458s, 1377m, 1302w, 1260m, 1194w, 1095m, 1034m, 951w, 870w, 851w, 800m, 722w, 674w, 620w, 571w, 444w ν(Y–O)
3	6.20 (s, 2 H)	5.50 (s, 4 H)	3.80 (s, 12 H, OMe), 3.85 (m, J = 7.0 Hz, 16 H, OCH_2)	1.24 (t, J = 7.0 Hz, 18 H, Me), 3.62 (m, J = 7.0 Hz, 12 H, CH_2), 2.60 (br., 6 H, OH)	3306 br ν(OH), 1631s, 1607s δ(OH), 1454s, 1398w, 1373w, 1349w, 1291m, 1242m, 1198m, 1078s, 1037s, 935s, 870s, 828m, 780w, 643m, 575m, 536m, 517m, 459m ν(Y–O)
4	5.40 (br., 2 H)	5.15 (s, 8 H)	3. 60 (br. m, 16 H, OMe of triglyme + OCH_2 of ethanol) 3.89 (br., 24 H, OCH_2)	1.18 (t, J = 7.0 Hz, 6 H, Me), 2.55 (br., 2 H, OH), 3. 60 (br. m, 16 H, OMe of triglyme + OCH_2 of ethanol)	3251 br ν(OH), 1617m δ(OH), 1464s, 1377m, 1349m, 1274m, 1239m, 1196m, 1090s, 1067s, 1019s, 993s, 946s, 876m, 833m, 718w, 632m, 456w ν(Y–O)
5	5.23, 5.35 (s, 2 H)	4.95 (br., 4 H)	3.60 (s, 12 H, OMe), 3.95 (m, J = 7.0 Hz, 32 H, OCH_2)	1.10 (t, J = 7.0 Hz, 6 H, Me), 2.61 (t, J = 7.0 Hz, 2 H, OH), 3.45 (m, J = 7.0 Hz, 4 H, CH_2)	3300, 3100 br ν(OH), 1602.2 m δ(OH), 1458s, 1377m, 1297m, 1273m, 1243m, 1201m, 1116s, 1091s, 1076s, 1027s, 950s, 910m, 875m, 853m, 792m, 718m, 679m, 625m, 571m, 454m ν(Y–O)

[a] ^{1}H NMR spectrum of **3** in CD_2Cl_2.

multiplicities and integrated intensity ratios (Table 2). The bridging hydroxo groups exhibit the greatest downfield shifting and appear as a singlet at δ = 5.40–6.40 ppm for compounds **1**–**4** but as two singlets (1:1) at δ = 5.23 and 5.35 ppm for compound **5**, probably as a result of some asymmetric interactions with the pendant oxygen atoms O5 and O5^i of the tetraglyme ligands in solution. The signals due to the coordinated water molecules appear as a relatively broad singlet in the region δ = 4.95–5.50 ppm. The signals of the methylene groups of glyme and coordinated ethanol are well resolved in the spectra of compounds **3** and **5** and show two distinct multiplets (J = 7 Hz) at δ = 3.85–3.95 and 3.45–3.62 ppm, respectively, while they appear as overlapping multiplets centered at δ = 3.60 ppm in the spectrum of complex **4**.

It is worth noting that some hydroxo-bridged dinuclear metal complexes have been shown to form dinuclear/mononuclear equilibrium mixtures in solution on the basis of their concentration-dependent NMR spectra.[25,26] The driving force for the formation of monomer units usually involves either the coordination of an additional Lewis base (e.g. R_3P) to the metal center[25] or the formation of new, stronger secondary hydrogen-bond interactions with the terminal metal hydroxide moiety.[26] Concentration-independent ^{1}H NMR spectra of **1**–**5** suggest that none of above-mentioned driving forces are important in the present case and indicate that the dimeric structure is probably retained upon dissolution.

Molecular Structures of $[Y_2(\mu\text{-}OH)_2(H_2O)_2(EtOH)_4(\eta^3\text{-diglyme})_2]I_4\cdot 2EtOH$ (3), $[Y_2(\mu\text{-}OH)_2(H_2O)_4(\eta^4\text{-triglyme})_2]I_4\cdot 2EtOH$ (4), and $[Y_2(\mu\text{-}OH)_2(H_2O)_2(EtOH)_2(\eta^4\text{-tetraglyme})_2]I_4$ (5)

The selected interatomic bond lengths and angles for compounds **3**, **4**, and **5** are given in Table 3, 4, and 5, respectively, whereas intramolecular hydrogen bond lengths are summarized in Table 6. All three structures are based on a centrosymmetric $Y_2(\mu\text{-}OH)_2$ diamond core (Figure 1). The oxygen atoms of the di-, tri-, or tetraglymes, ethanol and/or water molecules complete the eight-coordinate environment about each yttrium center in **3**–**5**. All iodides act as noncoordinating counteranions. Although all the yttrium centers in **3**–**5** are eight-coordinate, their stereochemistry is different. The geometry around yttrium in the $[Y_2(\mu\text{-}OH)_2(H_2O)_2(EtOH)_4(\eta^3\text{-diglyme})_2]^{4+}$ cation of (**3**·2EtOH) can best be described as a square antiprism, which is slightly distorted towards dodecahedral geometry (Figure 2).[27]

Table 3. Selected bond lengths and angles for $[Y_2(\mu\text{-}OH)_2(H_2O)_2(EtOH)_4(\eta^3\text{-diglyme})_2]I_4\cdot 2EtOH$ (**3**).

Bond lengths [Å]			
Y1–O6^i	2.246(6)	Y1–O6	2.223(6)
Y1–O7	2.425(6)	Y1–O2	2.364(6)
Y1–O3	2.471(6)	Y1–O5	2.494(6)
Y1–O4	2.440(6)	Y1–O1	2.386(6)
Bond angles [°]			
O6^i–Y1–O7	146.3(2)	O6^i–Y1–O5	85.8(2)
O6^i–Y1–O3	135.2(2)	O7–Y1–O5	67.7(2)
O7–Y1–O3	73.3(2)	O3–Y1–O5	102.5(2)
O6^i–Y1–O4	80.0(2)	O4–Y1–O5	65.0(2)
O7–Y1–O4	105.2(1)	O6–Y1–O5	143.7(2)
O3–Y1–O4	65.0(2)	O2–Y1–O5	136.1(2)
O6^i–Y1–O6	69.0(2)	O6^i–Y1–O1	74.7(2)
O7–Y1–O6	143.9(2)	O7–Y1–O1	79.7(2)
O3–Y1–O6	80.3(2)	O3–Y1–O1	150.0(2)
O4–Y1–O6	84.6(2)	O4–Y1–O1	136.8(2)
O6^i–Y1–O2	121.6(2)	O6–Y1–O1	116.8(2)
O7–Y1–O2	72.3(2)	O5–Y1–O1	78.6(2)
O3–Y1–O2	82.1(2)	O2–Y1–O1	77.3(2)
O4–Y1–O2	145.7(2)	Y1^i–O6–Y1	111.0(2)
O6–Y1–O2	80.1(2)		

Symmetry codes: (i) 2 –x, 1–y, 1–z.

The tridentate diglyme (O3, O4, and O5) and a water molecule (O7) occupy four adjacent corners of the square antiprism, the remaining sites being occupied by two ethanol molecules (O1 and O2) and the two bridging hydroxides (O6 and O6^{i}). The stereochemistry around the yttrium atoms in $[Y_2(\mu\text{-}OH)_2(H_2O)_4(\eta^4\text{-triglyme})_2]I_4\cdot 2EtOH$ (**4**) is slightly distorted dodecahedral (Figure 3).[27] The oxygen atoms of two bridging hydroxides (O5 and O5^{i}) and two water molecules (O6 and O7) form four corners of the first trapezoid, whereas the second trapezoid consists of four oxygen atoms, O1, O2, O3, and O4, of a triglyme ligand.

Table 4. Selected bond lengths and angles for $[Y_2(\mu\text{-}OH)_2(H_2O)_4(\eta^4\text{-triglyme})_2]I_4\cdot 2EtOH$ (**4**).

Bond lengths [Å]			
Y1–O5^{i}	2.262(4)	Y1–O2	2.447(4)
Y1–O5	2.237(4)	Y1–O3	2.500(4)
Y1–O7	2.386(4)	Y1–O4	2.387(4)
Y1–O6	2.372(4)	Y1–O1	2.420(4)
Bond angles [°]			
O5^{i}–Y1–O5	68.51(2)	O5^{i}–Y1–O4	87.89.8(1)
O1^{i}–Y1–O7	176.15(1)	O5–Y1–O4	98.98(1)
O5^{i}–Y1–O7	143.62(1)	O7–Y1–O4	88.61(1)
O5–Y1–O7	147.62(1)	O6–Y1–O4	81.29(2)
O5^{i}–Y1–O6	74.32(1)	O5^{i}–Y1–O1	83.46(1)
O5–Y1–O6	142.77(1)	O5–Y1–O1	90.1(1)
O7–Y1–O6	6936(1)	O2–Y1–O4	128.72(1)
O5^{i}–Y1–O2	136.49(1)	O3–Y1–O4	65.21(1)
O5–Y1–O2	81.61(1)	O2–Y1–O1	65.12(1)
O7–Y1–O2	69.43(1)	O3–Y1–O1	129.44(1)
O6–Y1–O2	127.14(1)	O4–Y1–O1	164.3(1)
O5^{i}–Y1–O3	135.1(1)	O6–Y1–O1	83.77(1)
O5–Y1–O3	80.5(1)	O2–Y1–O3	64.38(1)
O7–Y1–O3	74.2(1)	Y1^{i}–O5–Y1	111.49(2)
O6–Y1–O3	130.49(1)		

Symmetry codes: (i) $-x$, $1-y$, $1-z$.

Table 5. Selected bond lengths and angles for $[Y_2(\mu\text{-}OH)_2(H_2O)_2(EtOH)_2(\eta^4\text{-tetraglyme})_2]I_4$ (**5**).

Bond lengths [Å]			
Y1–O6^{i}	2.247(6)	Y1–O2	2.472(7)
Y1–O6	2.209(7)	Y1–O1	2.402(8)
Y1–O3	2.428(7)	Y1–O8	2.376(8)
Y1–O4	2.392(8)	Y1–O7	2.369(8)
Bond angles [°]			
O6^{i}–Y1–O6	67.3(3)	O6^{i}–Y1–O1	82.2(3)
O6^{i}–Y1–O3	139.3(3)	O6–Y1–O1	104.3(3)
O6–Y1–O3	79.2(2)	O3–Y1–O1	129.8(3)
O6^{i}–Y1–O4	90.8(3)	O4–Y1–O8	87.3(3)
O3–Y1–O4	66.0(3)	O2–Y1–O1	65.6(2)
O6–Y1–O4	89.9(3)	O1–Y1–O7	80.7(3)
O6^{i}–Y1–O2	126.5(3)	O8–Y1–O7	68.0(3)
O6–Y1–O2	80.4(3)	O1–Y1–O8	88.0(3)
O3–Y1–O2	65.8(2)	O2–Y1–O7	132.0(3)
O2–Y1–O8	77.4(3)	O4–Y1–O7	79.6(3)
O6^{i}–Y1–O7	77.6(3)	O4–Y1–O1	160.1(3)
O6^{i}–Y1–O8	145.4(3)	Y1^{i}–O3–Y1	112.7(3)
O3–Y1–O7	125.9(3)	O6–Y1–O8	147.2(3)
O3–Y1–O8	69.8(3)	O6–Y1–O7	143.2(2)
O4–Y1–O2	131.8(2)	Y1^{i}–O6–Y1	112.7(3)

Symmetry codes: (i) $-x$, y, $3/2-z$.

The yttrium centers in the complex $[Y_2(\mu\text{-}OH)_2(H_2O)_2(EtOH)_2(\eta^4\text{-tetraglyme})_2]I_4$ (**5**) have a bicapped trigonal prismatic geometry.[27] The six corners of the trigonal prism are occupied by the O1, O2, O4 (tetraglyme), O6, O6^{i} (bridging hydroxide), and O8 (ethanol) atoms, whereas O3 (tetraglyme) and O7 (water) atoms occupy the two capping positions (Figure 4).

Table 6. Intramolecular hydrogen bond lengths [Å] in **3**–**5**.

Compound **3**			
I1^{ii}···O1	3.444(7)	I2···O2	3.437(5)
I1^{ii}···O6^{i}	3.513(8)	I2···O7	3.501(8)
I1^{ii}···O3^{i}	3.934(8)	I2···O8^{iv}	3.470(1)
Compound 4			
I1···O6	3.443(5)	I2···O5	3.798(5)
I1···O7	3.505(5)	I2···O6^{i}	3.415(5)
Compound 5			
I1···O6^{i}	3.875(6)	I2···O3	3.761(7)
I1···O7	3.412(8)	I2···O8	3.441(8)

Symmetry codes, **3**: (i) $2-x$, $1-y$, $1-z$; (ii) $2-x$, $-y$, $-z$; (iv) $1-x$, $1-y$, $-z$. **4**: (i) $-x$, $1-y$, $1-z$. **5**: (i) $-x$, y, $3/2-z$.

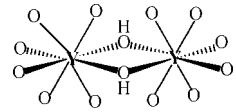

Figure 1. Coordination environment around yttrium centers in complexes **1**–**5**.

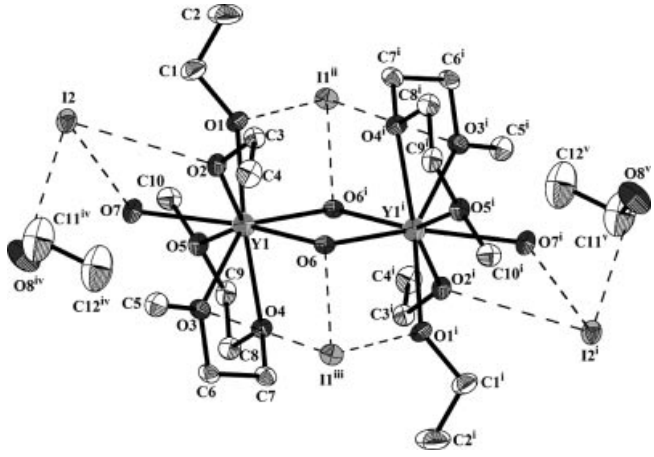

Figure 2. Molecular structure of $[Y_2(\mu\text{-}OH)_2(H_2O)_2(EtOH)_4(\eta^3\text{-diglyme})_2]I_4\cdot 2EtOH$ (**3**) with 30% ellipsoids. Hydrogen atoms have been omitted for clarity. Intramolecular hydrogen bonds are shown as broken lines (-----). Symmetry codes: (i) $2-x$, $1-y$, $1-z$; (ii) $2-x$, $-y$, $-z$; (iii) x, $1+y$, $1+z$; (iv) $1-x$, $1-y$, $-z$; (v) $1+x$, y, $1+z$.

Other than the stereochemistry, the structures of **3**–**5** appear to be affected only minimally by the change in the chelating glyme ligand. The average Y–O(glyme) bond lengths, decreasing slightly in the order diglyme (2.46 Å) > triglyme (2.44 Å) > tetraglyme (2.42 Å), are comparable with those in other yttrium complexes with glymes.[28] As expected, the average Y–O(μ-OH) length, 2.24 Å, is shorter than that of terminal Y–O (H_2O/EtOH), 2.38 Å. These values are consistent with those in the literature.[3b,12] Overall,

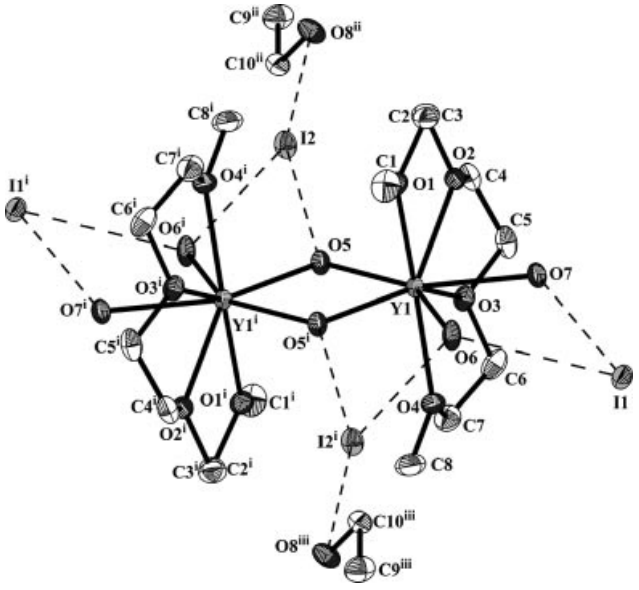

Figure 3. Molecular structure of $[Y_2(\mu\text{-}OH)_2(H_2O)_4(\eta^4\text{-triglyme})_2]I_4\cdot 2EtOH$ (**4**) with 30% ellipsoids. Hydrogen atoms have been omitted for clarity. Intramolecular hydrogen bonds are shown as broken lines (-----). Symmetry codes: (i) $-x, 1-y, 1-z$; (ii) $1-x, 1-y, 2-z$; (iii) $-1+x, y, -1+z$.

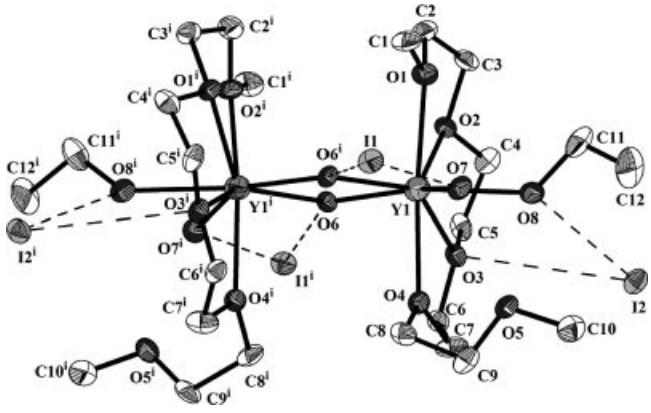

Figure 4. Molecular structure of $[Y_2(\mu\text{-}OH)_2(H_2O)_2(EtOH)_2(\eta^4\text{-tetraglyme})_2]I_4$ (**5**) with 30% ellipsoids. Hydrogen atoms have been omitted for clarity. Intramolecular hydrogen bonds are shown as broken lines (-----). Symmetry code: (i) $-x, y, 3/2-z$.

the Y–O bond lengths vary from 2.209(7) to 2.500(4) Å, the order of variation being Y–O(μ-OH) < Y–O(H_2O) ≈ Y–O(EtOH) < Y–O(glyme). The tetraglyme ligands in **5** are coordinated through four of their five oxygen atoms, the oxygen atoms, O5 and O5^i, lie too far away [4.116(9) Å] to interact with yttrium atoms (Figure 4). These pendant oxygen atoms, O5 and O5^i, are also far from the bridging hydroxide groups [4.811(1) Å]. The potentially pentadentate tetraglyme ligand has previously been shown to bind the metal centers in the η^3 or η^4 manner as well, depending upon steric considerations and the nature of metals.[29] The Y···Y distances [3.684(1)–3.719(1) Å] are also comparable with those reported for other hydroxo-bridged dinuclear yttrium complexes.[3b,12] In fact, a perusal of structural data for hydroxo-bridged dinuclear yttrium and lanthanide complexes with O- and N-donor ligands (Table 1) reveals that, despite differences in coordination number (7, 8, or 9), coordinating atoms (O and N), or central lanthanide atoms among these complexes, the dimensions of the $Ln_2(\mu\text{-}OH)_2$ diamond core vary little, as indicated by the small range of Ln···Ln [3.608(1)–3.988(1) Å] and Ln–μ-OH [2.19(1)–2.421(2) Å] distances as well as Ln–O–Ln angles [110.2(2)–112.7(3)°]. One additional feature of the $Y_2(\mu\text{-}OH)_2$ diamond core in the structures reported here is the presence of intramolecular hydrogen bonds between iodide anions and bridging hydroxide groups and coordinated water/ethanol molecules; the I···O distances vary in the range 3.412(8)–3.934(8) Å (Table 6). These distances are in agreement with those reported for hydrogen bonding involving iodides.[23]

$YBa_2Cu_3O_{7-x}$ (YBCO) Powder from $[Y_2(\mu\text{-}OH)_2(H_2O)_2(EtOH)_2(\eta^4\text{-tetraglyme})_2]I_4$ (5), $[Ba(tetraglyme)_2]I_2\cdot C_7H_8$, and CuI by Metal Organic Decomposition (MOD)

Iodides of yttrium, barium, and copper have been shown to be among the most attractive precursors for the formation of YBCO, since they do not form stable $BaCO_3$ during the decomposition.[1,30] However, formation of ionic Y-Cu clusters was recently reported by us from an all-iodide solution in DMF and 2-isopropoxyethanol.[23] This results in an inhomogeneous solution, which is inappropriate for MOD. The use of hydroxo-bridged dinuclear complex **5** instead of yttrium triiodide successfully suppressed this tendency, because of the presence of chelating glymes in the coordination sphere and also fewer iodide atoms than required for Y-Cu clusters. Another advantage of using derivatives $[Y_2(\mu\text{-}OH)_2(H_2O)_2(EtOH)_2(\eta^4\text{-tetraglyme})_2]I_4$ (**5**) and $[Ba(tetraglyme)_2]I_2\cdot C_7H_8$[31] as precursors is that they provide, as a result of their ionic nature, good solubility in ionic liquids (ILs). We then carried out the MOD process in high-boiling 1-butyl(methylimidazolium) bis[(trifluoromethyl)-sulfonyl]amide (IL) as the medium for the decomposition of an all-iodide solution containing $[Y_2(\mu\text{-}OH)_2(H_2O)_2(EtOH)_2(\eta^4\text{-tetraglyme})_2]I_4$ (**5**), $[Ba(tetraglyme)_2]I_2\cdot C_7H_8$, and CuI in the ratio 0.5:2:3. The as-prepared powder, after 1 h at 260 °C, was analyzed by FT-IR spectroscopy, TGA-DTA, and XRD. FT-IR data of the as-prepared powder show the presence of the tetraglyme ligand (1457m, 1351s, 1197s, 1138s, 791m cm^{-1}) and other absorption bands corresponding to ν(OH) (3470br cm^{-1}) and ν(Y–O) (678m, 572m, 514m cm^{-1}). No absorption bands characteristic of the IL could be observed. The TGA and DTA patterns (Figure 5) of this powder showed a two-step decomposition process in the range 270–420 °C associated with strong exothermic peaks corresponding to the combustion of the remaining organics. The total weight loss was 65.5%. The as-prepared powder was amorphous, and crystallization of the $YBa_2Cu_3O_{6.35}$ phase started after annealing in air at only 500 °C. This temperature is much lower than that reported for YBCO powder/films obtained from trifluoroacetate derivatives.[32] XRD analysis of the sample annealed at 900 °C showed the well-crystallized $YBa_2Cu_3O_{6.35}$ phase (Fig-

ure 6), though some additional peaks indexing as $YBa_2Cu_4O_8$ were also observed. Crystallite sizes of 25–44 nm were calculated by using the Debye–Scherrer formula. To the best of our knowledge, this is the first report of the use of a neat ionic liquid for synthesis of a high T_c superconductor material.[33]

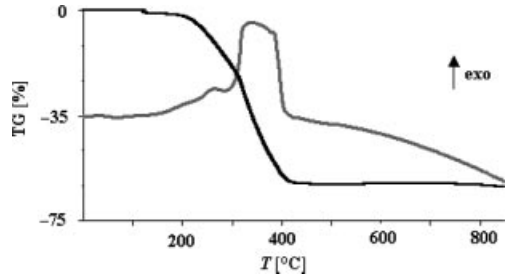

Figure 5. TGA-DTA curve of the powder obtained from the MOD of $[Y_2(\mu\text{-}OH)_2(H_2O)_2(EtOH)_2(\eta^4\text{-tetraglyme})_2]I_4$ (**5**), $[Ba(tetraglyme)_2]I_2{\cdot}C_7H_8$, and CuI.

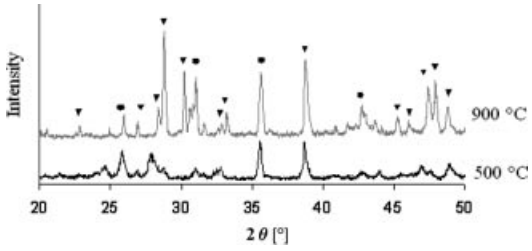

Figure 6. XRD of the powder obtained from the MOD of **5**, $[Ba(tetraglyme)_2]I_2{\cdot}C_7H_8$, and CuI (▼ = $YBa_2Cu_3O_{6.35}$ phase; ■ = $YBa_2Cu_4O_8$ phase).

Conclusion

We described here a facile synthetic route to ionic, centrosymmetric, hydroxo-bridged, dimeric yttrium iodide complexes with glymes. It is the first report of hydroxo-bridged dimeric yttrium (or lanthanide) complexes with an all-oxygen environment. Such dimeric hydroxo species are potentially good starting materials for the synthesis of larger yttrium oxo/hydroxo clusters. Unlike yttrium triiodide, use of these dinuclear yttrium hydroxo iodide species in an all-iodide solution for high T_c superconductors successfully suppresses the formation of ionic Y–Cu species and thus provides a homogeneous solution for MOD. Preliminary studies show that the $YBa_2Cu_3O_{6.35}$ phase starts after annealing the as-prepared powder in air at 500 °C, though some additional peaks indexing as $YBa_2Cu_4O_8$ were also observed. Further studies are now in progress to obtain the desired $YBa_2Cu_3O_{7-x}$ phase only.

Experimental Section

All reactions were carried out under argon by using Schlenk tubes and vacuum line techniques. $Y(i\text{PrOH})_4I_3$[22] and $[Ba(tetraglyme)_2]I_2{\cdot}C_7H_8$[31] were prepared as reported, whereas CuI was purchased from Aldrich Co. and used as received. Solvents were purified by standard methods. Di-, tri-, and tetraglyme (Aldrich) were stored over molecular sieves. The ionic liquid 1-butyl(methylimidazolium) bis[(trifluoromethyl)sulfonyl]amide was purchased from Solvionic and used without purification. ^{1}H NMR spectra were registered with a Bruker AC-300 spectrometer. FT-IR spectra of **1**–**5** were recorded as Nujol mulls with a Perkin–Elmer Paragon 500 spectrometer, whereas IR spectra of YBCO powder were recorded as KBr pellets with a Bruker Vector-22 spectrometer. TGA/DTA data were collected with a Setaram 92 system in air (thermal ramp 10 °C/min, 20–900 °C). XRD were obtained with a Bruker (Siemens) D 500 diffractometer by using Cu-K_α radiation. Analytical data were obtained from the Service Central d′Analyses du CNRS.

Synthesis of Compounds 1–5

$[Y_2(\mu\text{-}OH)_2(H_2O)_2(i\text{PrOH})_2(\text{triglyme})_2]I_4$ (1): Addition of a toluene solution (5 mL) of triglyme (0.5 mL) and H_2O (47 μL, 2.65 mmol) to a suspension of $Y(i\text{PrOH})_4I_3$ (0.94 g, 1.32 mmol) in toluene (3 mL) led to an immediate precipitation of a yellow-orange solid. After the mixture was stirred at room temp. for 6 h, the precipitate was separated by filtration and washed twice with *n*-hexane. Crystallization by slow cooling of a hot 2-propanol solution of this solid gave needle-shaped crystals, which were unsuitable for X-ray crystallography (0.62 g, 77%). $C_{22}H_{58}I_4O_{14}Y_2$ (1231.4): calcd. C 21.43, H 4.71; found C 21.82, H 4.54.

$[Y_2(\mu\text{-}OH)_2(H_2O)_2(\text{tetraglyme})_2]I_4$ (2): With the same procedure, **2** was obtained from $Y(i\text{PrOH})_4I_3$ (0.99 g, 1.38 mmol), tetraglyme (0.3 mL) and H_2O (50 μL, 2.78 mmol) in toluene (10 mL) as a yellow solid and crystallized by slow cooling of its hot 2-propanol solution (0.61 g, 73%). $C_{20}H_{25}I_4O_{14}Y_2$ (1199.4): calcd. C 20.01, H 4.16; found C 19.17, H 4.16.

$[Y_2(\mu\text{-}OH)_2(H_2O)_2(EtOH)_4(\eta^3\text{-diglyme})_2]I_4{\cdot}2EtOH$ (3): An ethanol (5 mL) solution of diglyme (0.4 mL) and H_2O (27 μL, 1.49 mmol) was added to a solution of $Y(i\text{PrOH})_4I_3$ (0.55 g, 0.77 mmol) in EtOH (5 mL), and the resulting solution was stirred at room temp. for 6 h. Removal of solvents under vacuum afforded **3** as a yellow solid, which was crystallized from EtOH/*n*-pentane (1:1) at room temp. (0.74 g, 74%). $C_{24}H_{70}I_4O_{16}Y_2$ (1300.3): calcd. C 22.15, H 5.38; found C 21.93, H 5.27.

$[Y_2(\mu\text{-}OH)_2(H_2O)_4(\eta^4\text{-triglyme})_2]I_4{\cdot}2EtOH$ (4): This compound was obtained as yellow solid by using the same procedure from $Y(i\text{PrOH})_4I_3$ (0.71 g, 1.0 mmol), triglyme (0.5 mL), and H_2O (55 μL, 3.05 mmol) in ethanol (5 mL) followed by crystallization from EtOH/*n*-pentane (1:1) at –20 °C (0.81 g, 68%). $C_{20}H_{54}I_4O_{14}Y_2$ (1238.1): calcd. C 19.90, H 4.47; found C 19.78, H 4.41. Compound **4** was also obtained by crystallization of **1** from EtOH/*n*-pentane (1:1) at –20 °C in 60% yield.

$[Y_2(\mu\text{-}OH)_2(H_2O)_2(EtOH)_2(\eta^4\text{-tetraglyme})_2]I_4$ (5): In a similar procedure, the reaction of $Y(i\text{PrOH})_4I_3$ (0.69 g, 0.97 mmol) with tetraglyme (0.5 mL) and H_2O (35 μL, 1.94 mmol) in ethanol (5 mL) followed by crystallization from EtOH/Et_2O (1:2) at –20 °C afforded $[Y_2(\mu\text{-}OH)_2(H_2O)_2(EtOH)_2(\eta^4\text{-tetraglyme})_2]I_4$ (**5**) as a pale yellow crystalline solid (0.87 g, 70%). $C_{24}H_{62}I_4O_{16}Y_2$ (1292.2): calcd. C 22.29, H 4.79; found C 22.11, H 4.72. Compound **5** was also obtained by crystallization of **2** from EtOH/Et_2O (1:2) at –20 °C in 57% yield.

Compounds **1**–**5** are yellow or orange-yellow solids, insoluble in aliphatic or aromatic hydrocarbons but soluble in acetonitrile and ethanol. They are only moderately soluble in 2-propanol and dichloromethane.

Preparation of $YBa_2Cu_3O_{7-x}$ (YBCO) Powder from $[Y_2(\mu\text{-}OH)_2(H_2O)_2(EtOH)_2(\eta^4\text{-tetraglyme})_2]I_4$, $[Ba(tetraglyme)_2]I_2{\cdot}C_7H_8$, and CuI by Metal Organic Decomposition

$[Y_2(\mu\text{-}OH)_2(H_2O)_2(EtOH)_2(\eta^4\text{-tetraglyme})_2]I_4$ (0.54 g, 0.42 mmol) and $[Ba(tetraglyme)_2]I_2{\cdot}C_7H_8$ (1.55 g, 1.66 mmol) were each dissolved in ethanol (5 mL). Dissolution of CuI (0.47 g, 2.50 mmol) in ethanol (5 mL) was achieved by using a solution of NH_4I in ethanol (3.4 M, 3 mL). Mixing of these solutions gave an orange-yellow clear solution. After addition of the ionic liquid 1-butyl-(methylimidazolium) bis[(trifluoromethyl)sulfonyl]amide (10 mL) into this solution, ethanol was removed under vacuum to give a yellow pasty liquid. After this solution was heated at 260 °C for 1 h, the brownish-black powder was precipitated by adding methanol (30 mL). This powder was then removed by centrifugation and washed twice with hexane (0.36 g).

X-ray Crystallography

Suitable crystals of **3**–**5** were obtained from EtOH/pentane (1:1, room temp. or –20 °C) or EtOH/Et_2O (1:2, –20 °C) solutions and mounted on a Nonius Kappa CCD diffractometer with Mo-K_α radiation (λ = 0.71073 Å). Crystallographic and refinement data for **3**–**5** are given in Table 7. Intensities were collected at 150 K by means of the program COLLECT.[34] Reflection indexing, Lorentz-polarization correction, peak integration, and background determination were carried out with the DENZO program.[35] Frame scaling and refinement of unit-cell parameters were carried out with the program SCALEPACK.[35] Absorption correction was achieved with the program DIFABS.[36] The starting structure was solved by direct methods with SIR92.[37] The remaining non-hydrogen atoms were located by successive difference Fourier map analyses. The structure refinement was carried out with CRYSTALS.[38] The H atoms were placed geometrically and refined with riding constraints.

Table 7. Crystallographic and refinement data for **3**–**5**.

Compound	**3**	**4**	**5**
Empirical formula	$C_{24}H_{70}I_4O_{16}Y_2$	$C_{20}H_{56}I_4O_{16}Y_2$	$C_{24}H_{62}I_4O_{16}Y_2$
Formula weight	1300.3	1238.1	1292.2
Crystal system	triclinic	triclinic	monoclinic
Space group	$P\bar{1}$	$P\bar{1}$	$C2/c$
a [Å]	11.04(5)	9.88(5)	23.48(5)
b [Å]	11.08(5)	10.62(5)	12.00(5)
c [Å]	1I.54(5)	11.45(5)	15.89(5)
α [°]	111.91(5)	64.96(5)	90
β [°]	95.77(5)	85.22(5)	88.51(5)
γ [°]	111.86(5)	72.15(5)	90
Volume [Å^3]	1167.8(9)	1035.9(8)	4477(3)
Z	1	1	4
Absorption coefficient [mm^{-1}]	5.17	5.82	5.39
Temperature [K]	150	150	150
Measured reflections	15019	12822	15104
Independent reflections	5567	4918	3974
R_{int}	0.139	0.070	0.147
Data/restrains/parameters	3467/7/208	3233/0/190	2123/0/208
Goodness of fit	1.11	1.08	1.10
R_1 [I>2(σ)]	0.0347	0.0350	0.0602
R_1 (all data)	0.0665	0.0556	0.1292
wR_2 [I>2(σ)]	0.0389	0.0416	0.0492
wR_2 (all data)	0.0574	0.0543	0.0742
Residual electron density [e Å^{-3}]	–1.98 to 2.57	–1.33 to 1.13	–0.92 to 1.26

CCDC-628903–628905 contain the supplementary crystallographic data for **3**–**5**. These data can be obtained free of charge from The Cambridge Crystallographic Data Centre via www.ccdc.cam.ac.uk/data_request/cif.

Acknowledgments

S. M. is grateful to the region Rhone Alpes for a postdoctoral fellowship (project Superflex).

[1] a) R. H. Baney, D. F. Bergstrom, B. H. Justice, *Chem. Mater.* **1992**, *4*, 984–987; b) I. Matsubara, M. Paranthaman, A. Singhal, C. Vallet, D. F. Lee, P. M. Martin, R. D. Hunt, R. Feenstra, C. Y. Yang, S. E. Babcock, *Physica C* **1999**, *319*, 127–132.
[2] L. G. Hubert-Pfalzgraf, *New J. Chem.* **1987**, *11*, 663–675.
[3] See for example: a) S. J. Oh, K. H. Song, D. Whang, K. Kim, T. H. Yoon, H. Moon, J. W. Park, *Inorg. Chem.* **1996**, *35*, 3780–3785; b) S. W. A. Bligh, N. Choi, E. G. Evagorou, M. McPartlin, K. N. White, *J. Chem. Soc., Dalton Trans.* **2001**, 3169–3172; c) F. Aguilar-Perez, P. Gomez-Tagle, E. Collado-Fregoso, A. K. Yatsimirsky, *Inorg. Chem.* **2006**, *45*, 9502–9517.
[4] A. Domingos, M. R. J. Elsegood, A. C. Hillier, G. Lin, S. Y. Liu, I. Lopes, N. Marques, G. Maunder, R. McDonald, A. Sella, J. W. Steed, J. Takats, *Inorg. Chem.* **2002**, *41*, 6761–6768.
[5] R. Wang, H. Liu, M. D. Carducci, T. Jin, C. Zheng, Z. Zheng, *Inorg. Chem.* **2001**, *40*, 2743–2750.
[6] a) R. Wang, M. D. Carducci, Z. Zheng, *Inorg. Chem.* **2000**, *39*, 1836–1837; b) N. Mahe, O. Guillou, C. Daiguebonne, Y. Gerault, A. Caneschi, C. Sangregorio, J. Y. Chane-Ching, P. E. Car, T. Roisnel, *Inorg. Chem.* **2005**, *44*, 7743–7750; c) A.-V. Mudring, T. Timofte, A. Babai, *Inorg. Chem.* **2006**, *45*, 5162–5166.
[7] R. Wang, H. D. Selby, H. Liu, M. D. Carducci, T. Jin, Z. Zheng, J. W. Anthis, R. J. Staples, *Inorg. Chem.* **2002**, *41*, 278–286.
[8] R. Anwander, *Angew. Chem. Int. Ed.* **1998**, *37*, 599–602.
[9] Z. Zheng, *Chem. Commun.* **2001**, 2521–2529.
[10] L. G. Hubert-Pfalzgraf, L. Cauro-Gamet, A. Brethon, S. Daniele, P. Richard, *Inorg. Chem. Commun.* **2007**, *10*, 143–147.
[11] L. G. Hubert-Pfalzgraf, N. Miele-Pajot, R. Papienik, J. Vaissermann, *J. Chem. Soc., Dalton Trans.* **1999**, 4127–4130.
[12] M. D. Grillone, F. Benetollo, G. Bombieri, *Polyhedron* **1991**, *10*, 2171–2177.
[13] W. J. Evans, G. W. Rabe, J. W. Ziller, *Inorg. Chem.* **1994**, *33*, 3072–3078.
[14] S. Petoud, J.-C. G. Bünzli, F. Renaud, C. Piguet, K. J. Schenk, G. Hopfgartner, *Inorg. Chem.* **1997**, *36*, 5750–5760.
[15] R. Wang, J. Zhao, T. Jin, G. Xu, Z. Zhou, X. Zhou, *Polyhedron* **1998**, *17*, 43–47.
[16] W.-K. Wong, L. Zhang, F. Xue, T. C. W. Mak, *J. Chem. Soc., Dalton Trans.* **1999**, 3053–3062.
[17] E. Baraniak, R. S. L. Bruce, H. C. Freeman, N. J. Hair, J. James, *Inorg. Chem.* **1976**, *15*, 2226–2230.
[18] Y.-Q. Zheng, L.-X. Zhou, J.-L. Lin, S.-W. Zhang, *Z. Anorg. Allg. Chem.* **2001**, *627*, 2425–2429.
[19] D.-Y. Wei, Y.-Q. Zheng, J.-L. Lin, *Z. Naturforsch., Teil B* **2002**, *57*, 625–630.
[20] L. Natrajan, J. Pécaut, M. Mazzanti, C. LeBrun, *Inorg. Chem.* **2005**, *44*, 4756–4765.
[21] L. Natrajan, J. Pécaut, M. Mazzanti, *Dalton Trans.* **2006**, 1002–1005.
[22] S. Mishra, L. G. Hubert-Pfalzgraf, M. Rolland, H. Chermette, *Inorg. Chem. Commun.* **2007**, *10*, 15–19.
[23] S. Mishra, L. G. Hubert-Pfalzgraf, E. Jeanneau, H. Chermette, *Dalton Trans.* **2007**, 410–413.
[24] W. Teng, M. Guino-o, J. Hitzbleck, U. Englich, K. Ruhlandt-Senge, *Inorg. Chem.* **2006**, *45*, 9531–9539.
[25] V. V. Grushin, H. Alper, *Organometallics* **1996**, *15*, 5242–5245.
[26] R. A. Allred, S. A. Huefner, K. Rudzka, A. M. Arif, L. M. Berreau, *Dalton Trans.* **2007**, 351–357.
[27] a) C. W. Haigh, *Polyhedron* **1995**, *14*, 2871–2878; b) C. W. Haigh, *Polyhedron* **1996**, *15*, 605–643.

[28] a) S. R. Drake, M. B. Hursthouse, K. M. A. Malik, S. A. S. Miller, D. J. Otway, *Inorg. Chem.* **1993**, *32*, 4464–4471; b) K. D. Pollard, J. J. Vittal, G. P. A. Yap, R. J. Puddephatt, *J. Chem. Soc., Dalton Trans.* **1998**, 1265–1267; c) G. Malandrino, R. L. Nigro, I. L. Fragala, C. Benelli, *Eur. J. Inorg. Chem.* **2004**, 500–509.
[29] a) S. R. Drake, S. A. S. Miller, D. J. Williams, *Inorg. Chem.* **1993**, *32*, 3227–3235; b) M. E. Fragala, G. Malandrino, O. Puglist, C. Benelli, *Chem. Mater.* **2000**, *12*, 290–293.
[30] L. C. Pathak, S. K. Mishra, *Supercond. Sci. Technol.* **2005**, *18*, R67–R89.
[31] S. Mishra, L. G. Hubert-Pfalzgraf, E. Jeanneau, *Polyhedron* **2007**, *26*, 66–72.
[32] T. Araki, I. Hirabayashi, *Supercond. Sci. Technol.* **2003**, *16*, R71–R94.
[33] A. Taubert, Z. Li, *Dalton Trans.* **2007**, 723–727.
[34] B. V. Nonius, *COLLECT*, Delft, The Netherlands, **1997**–2001.
[35] Z. Otwinowski, W. Minor, *Methods in Enzymology* (Eds.: C. W. Carter Jr, R. M. Sweet), New York, Academic Press, **1997**, vol. 276, pp. 307–326.
[36] N. Walker, D. Stuart, *Acta Crystallogr., Sect. A* **1983**, *39*, 158–166.
[37] A. Altomare, M. C. Burla, M. Camalli, G. L. Cascarano, C. Giacovazzo, A. Guagliardi, A. G. G. Moliterni, G. Polidori, R. Spagna, *J. Appl. Crystallogr.* **1999**, *32*, 115–119.
[38] P. W. Betteridge, J. R. Carruthers, R. I. Cooper, K. Prout, D. J. Watkin, *J. Appl. Crystallogr.* **2003**, *36*, 1487.

Received: December 22, 2006
Published Online: April 4, 2007

